

Stable Ti/TaSi₂/Pt Ohmic Contacts on N-Type 6H-SiC Epilayer at 600°C in Air

Robert S. Okojie¹, David Spry², Jeff Krotine², Carl Salupo², and Donald R. Wheeler¹

¹NASA Glenn Research Center, Instrumentation and Controls Division
21000 Brookpark Road, M/S 77-1, Cleveland OH 44135; (216) 433-6522

²Akima Corporation, Fairview Park, OH 44126.

ABSTRACT

We report preliminary electrical and diffusion barrier characteristics of Ti (100nm)/TaSi₂ (200nm)/Pt (300nm) thermally stable ohmic contact metallization on n-type 6H-SiC epilayers. These contacts exhibited linear ohmic characteristics with contact resistance in the range of $(0.3 \times 10^{-4} - 8 \times 10^{-4}) \Omega\text{-cm}^2$ on n-type epilayer doped between 0.6 to $2 \times 10^{19} \text{cm}^{-3}$. The I-V characteristics and contact resistance remained stable after heat treatments at 500°C and 600°C in air for over 600 hours and 150 hours, respectively. Auger Electron Spectroscopy (AES) was used to analyze the metal and semiconductor interfaces to understand the prevailing reactions. The thermal stability of the ohmic contact between 500°C and 600°C in air is believed to be due to the formation of silicides and carbides of titanium after being annealed at 600°C in H₂ (5%)/N₂ forming gas for 30 minutes. The oxidation of silicon species that migrated after TaSi₂ decomposition is proposed as the diffusion barrier mechanism.

INTRODUCTION

There is growing demand for devices to operate in higher temperature environments (>500°C) beyond the capability of silicon and gallium arsenide technology. Most existing electronic devices are limited to temperatures below 200°C, primarily due to the degradation of the intrinsic properties of the associated materials (silicon and gallium arsenide) [1, 2]. Silicon-on-Insulator (SOI) technology was developed to extend device operation to about 300°C [3]. However, long-term SOI reliability beyond this temperature remains unproven. Silicon carbide (SiC) based technology appears to be the most technologically mature among wide bandgap semiconductors with the proven capability to function at temperatures above 500°C [4,5]. However, contact metallization of SiC undergoes severe degradation beyond this temperature due to enhanced thermochemical reactions and microstructural changes that lead to device failure and thereby limiting device functional capability. The causative factors of contact failures include inter-diffusion between layers, oxidation and compositional and microstructural changes. These mechanisms are potential device killers by way of contact failure [6]. Liu and Papanicolaou [7,8] have, respectively, demonstrated stable ohmic contacts at 650°C for up to 3000 hours and 850°C for a short duration in vacuum. Vacuum aging is, however, not representative of the environmental condition these devices are expected to operate in.

The research presented here is part of an on-going effort to develop high reliability contact metallization schemes capable of supporting various SiC sensors and electronics within the temperature range of 500°C and 600°C in air. Such schemes are expected to have the following attributes: (a) Ohmic contact with reasonably low contact resistance relative to the bulk epilayer; (b) Long-term contact stability in the harsh environment; (c) Compatibility with SiC large-scale integrated fabrication technology; (d) Good wirebond strength; and (e) Compatibility with high temperature interconnect and packaging technology.

EXPERIMENT

Several (0001)-oriented (3.5° off-axis), high resistivity, Si-face, p-type 6H-SiC substrates each having $0.5\ \mu\text{m}$ thick n-type epilayer of different doping levels were commercially obtained from Cree Research [9]. The wafers were inspected as received and the surface features mapped with a Nikon high-resolution Nomarski optical microscope. Then an oxidation and etching processes described in [10] was used to create the circular contact holes. The sample was then loaded into the deposition chamber. An in-situ dehydration process in vacuum at 300°C for one hour was followed by *in-vacuo* sequential deposition of Ti (100nm)/TaSi₂ (200nm)/Pt (300nm) in a three-gun, UHV/load-load, sputtering system. Details of the deposition parameters are shown in Table 1. A 2- μm aluminum layer was deposited by e-beam evaporation and used as an etch mask during reactive ion etching (RIE) to pattern the Shockley probe pads over the contacts, which makes probing easier, and also protect the contacts.

Table 1: Process parameters for the deposition of Ti/TaSi₂/Pt.

Layer	Thickness(nm)	Deposition conditions				
		Pressure	Power (W)	Gas flow (sccm)	Time (min.)	Deposition Method
Ti	100	6 mTorr	200 R.F.	50 Ar	16.5	Sputtering
TaSi ₂	200	6mTorr	100 R.F.	50 Ar	33.3	“
Pt	300	9mTorr	75 D.C.	50 Ar	6.3	“

Following the RIE, aluminum was selectively etched in an aluminum etchant to expose the platinum layer. The final configuration of the contact is shown in figure 1, which is similar to the conventional four-point probe. Constant current, I_{AD} , is passed from pad A and out through pad D. The voltage, V_{BC} , measures the voltage between pad B and C, which makes it possible to calculate the resistance of the epilayer segment between the two contacts, and also the sheet resistance by using epilayer thickness and resistivity. The voltage, V_{AB} , measures the voltage across the segment between pad A and B, which includes the spreading resistance. Auger electron spectroscopy (AES) depth profiling was used to analyze the contacts at various stages of thermal treatment in a high temperature oven.

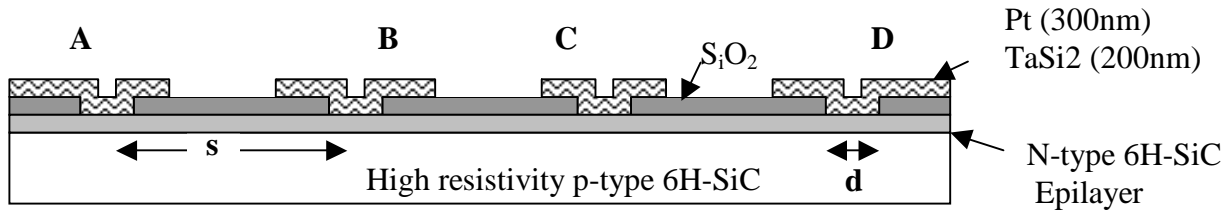


Figure 1: Cross section view of four-point probe configuration used for this experiment.

Two batches of samples prepared from the same wafer (net epilayer doping, $N_d = 2 \times 10^{19}\ \text{cm}^{-3}$) were used for this experiment. The two batches were metallized in different deposition runs. The batch labeled CRA was metallized first. The AES depth profile analysis of the metallization on this batch showed an unusually high concentration of oxygen at the Ti/TaSi₂ (~5 at. %) and TaSi₂/Pt (~3 at. %) interfaces. This led to some interfacial delamination. After the oxygen contamination was

contained, the second sample batch, labeled CRD was then metallized. The two batches were then both annealed at the same time in a tube furnace at 600°C for 30 minutes in H₂/N₂. Sample set CRA was then treated at 500°C while sample set CRD was treated at 600°C, all in air. The samples were intermittently cooled down to room temperature to allow for measuring the I-V characteristics and specific contact resistance. They were heated back to their respective temperatures after each measurement. The specific contact resistance, ρ_{cs} , was calculated using the modified four-point probe method with equation expressed as [11]:

$$\rho_{cs} = \frac{A}{I_{AD}} \left[V_{AB} - V_{BC} \frac{\ln \left(\left(3 \frac{s}{d} \right) - \left(\frac{1}{2} \right) \right)}{2 \ln 2} \right] [\Omega \cdot \text{cm}^2] \quad (1)$$

where A is the area under the contact (cm)², s is the center-to-center separation between contacts (cm), d is the contact diameter (cm), and I_{AD} is the constant current, which in this case was 0.5mA. As a result of this modification, the result obtained using equation (1) would give slightly higher specific contact resistance values than that of the unmodified equation, since it also takes into consideration the spreading resistance. One primary interest of this overall research is to understand how the contact resistance, including the spreading resistance would change to affect device functionality.

RESULTS AND DISCUSSION

The specific contact resistances as function of time at temperature of the two sets are shown in figures 2a and b. The samples treated at 500°C, shown in figure 2a, exhibited higher contact resistance values initially and remained high for the first forty hours. These values, however, dropped after then and

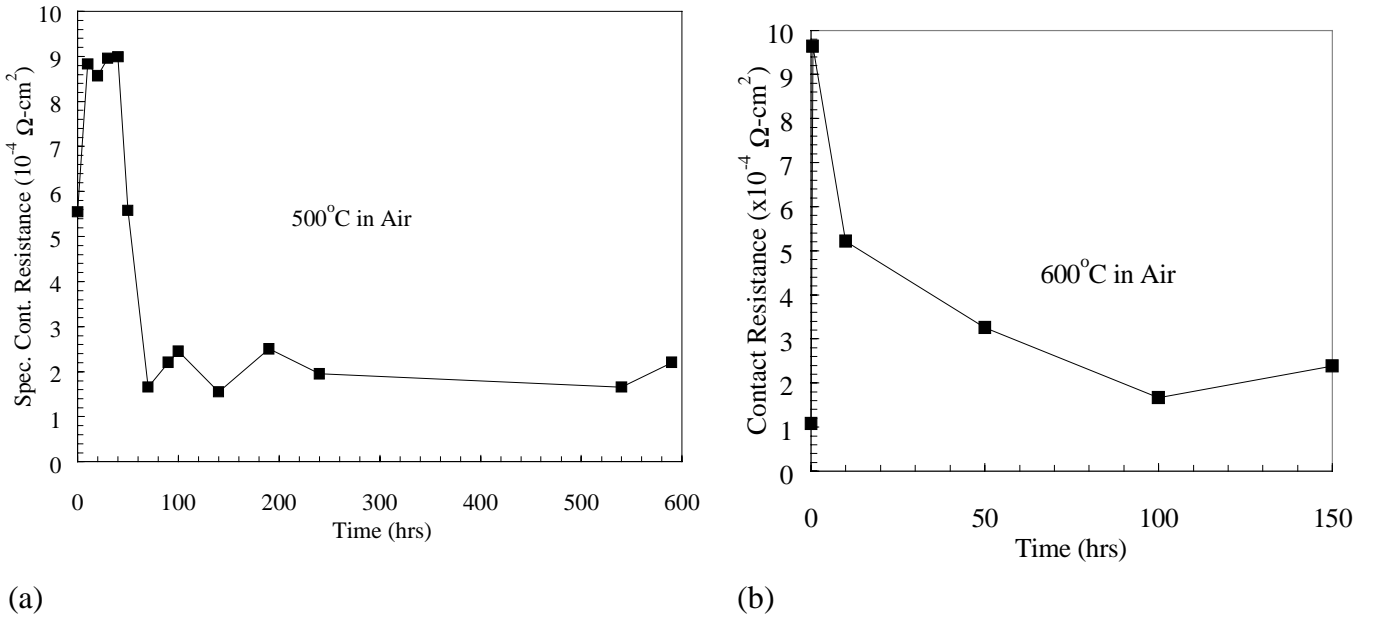


Figure 2: Average specific contact resistance as a function of time after (a) 500°C in air. The high contact resistance in the first few hours may be attributed to conditions stated in the text; (b) 600°C in air.

practically remained constant between 70 and over 600 hours. The result of the set tested at 600°C in air for 150 hours is shown in figure 2b. The specific contact resistance also increased after the initial 30-minute anneal at 600°C in the forming gas. Subsequent heat treatments in air, however, saw an exponential decrease of the contact resistance values and appeared to taper off after 100 hours.

There is an obvious difference in the contact resistance values between the two sample sets in the first forty hours as depicted in figures 2a and 2b. This observed differences in contact resistance values could be attributed to one or a combination of three things: (a) the oxygen contamination of samples treated at 500°C in air; (b) the probable existence of surface states; and (c) incomplete reaction product formation at the SiC interface after initial 30 minutes anneal at 600°C in forming gas which might be accelerated by the subsequent heat treating at 600°C. Although the oxygen contamination was eliminated prior to the metallization of sample set treated at 600°C in air, we could not conclude with certainty that oxygen contamination was solely responsible for the observed initial differences in contact resistance values. Since the heat treatments in air between the sample sets are different, variations in activation energies may cause differences in product formation, thereby leading to variations in electrical characteristics. After the initial contrast in results between both sample sets, the average specific contact resistance for either set leveled off to values ranging between $2\text{-}3 \times 10^{-4} \Omega\text{-cm}^2$.

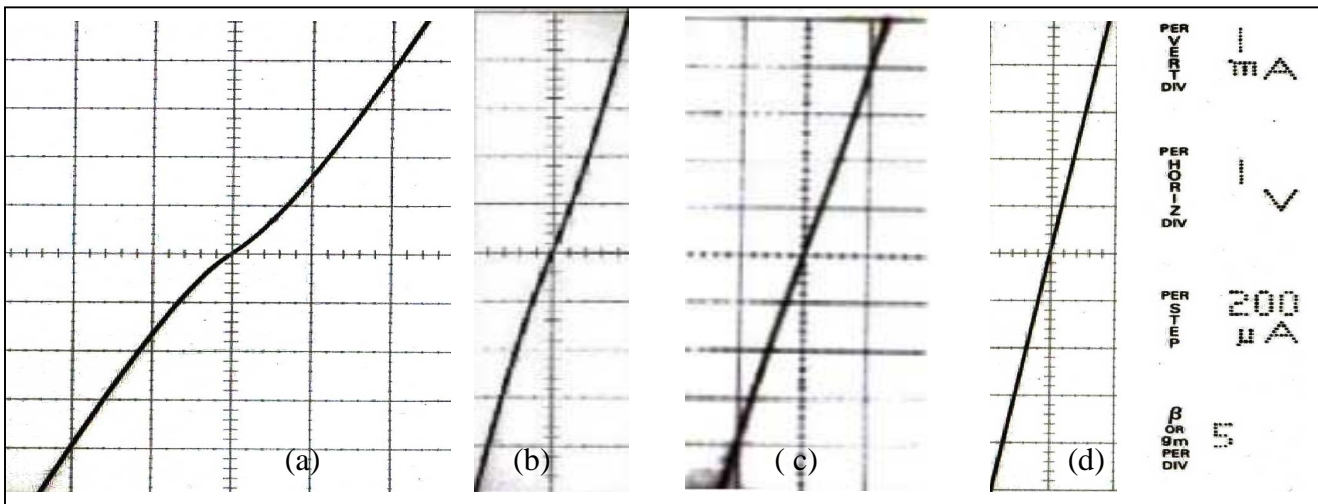


Figure 3: I-V characteristics of samples measured at different stages: (a) as-deposited, (b) 600°C annealed in H_2 (5%)/ N_2 forming gas for 30 minutes, (c) sample treated at 500°C in air for 630 hours, and (d) sample treated at 600°C in air for 150 hours. Note the scaling is the same for all.

The representative I-V characteristics after various conditions for both sets of samples are shown in figure 3. The I-V curve shown in figure 3a is that of the as-deposited condition, which was the same for both sample sets. The observed weak rectification could be related to low level oxidation issues already discussed above. The entire sample set exhibited linear I-V characteristics after annealing at 600°C in H_2 (5%)/ N_2 forming gas for 30 minutes, as shown in figure 3b. The slight curvature observed could only be attributed to the on-going reaction at the SiC interface. Figure 3c shows that the representative I-V characteristic of the sample set after 630 hours at 500°C in air remained practically unchanged relative to figure 3b. The observed slight change in the I-V slope was an artifact of the oxidation process occurring on the Shockley pads, which required scratching the surface with the probe tips before good electrical probe contact was made. For the sample set treated

at 600°C in air, the slope of the I-V characteristic after 150 hours, shown in figure 3d, compares very well with that of figures 3b and c. This could be expected given that they were both from the same wafer (net epilayer doping level, $N_d = 2 \times 10^{19} \text{ cm}^{-3}$) and is an indication of the thermal stability of the new SiC interface even with the slight difference in processing conditions.

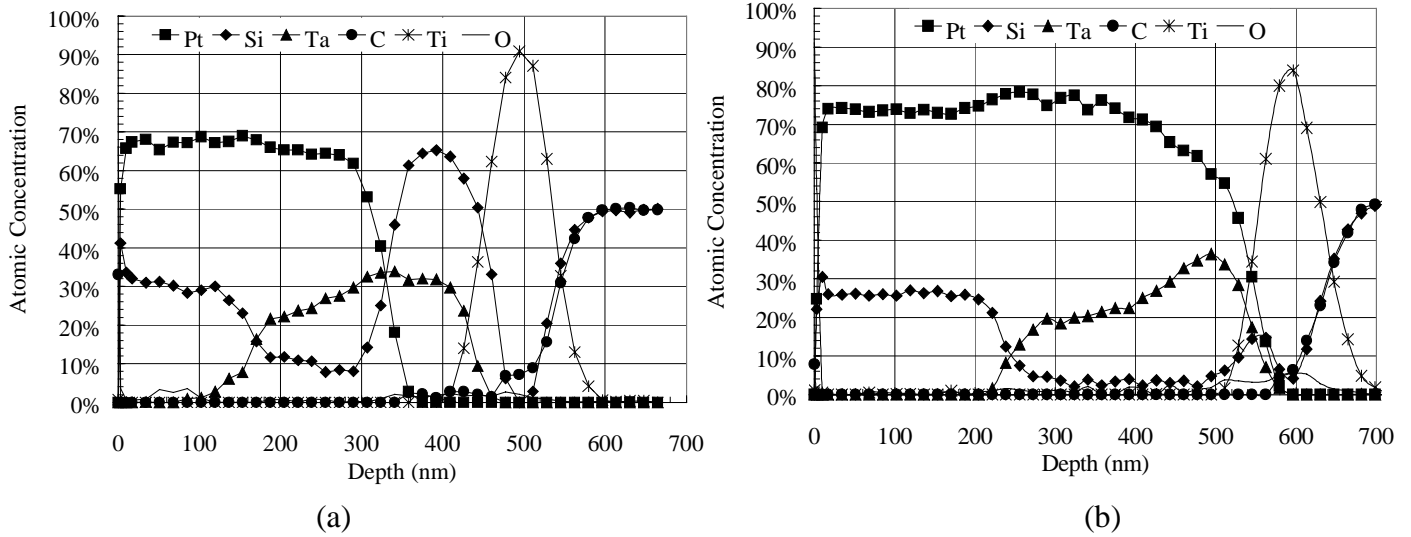


Figure 4: Auger depth profile of 6H-SiC/Ti/TaSi₂/Pt after heat treatments at: (a) 600°C anneal in H₂ (5%) /N₂ 30 minutes, and (b) 500°C treatment in air for fifty hours.

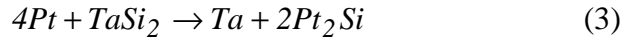
To begin understanding of the active mechanisms, we examined the relationship between the electrical and thermochemical characteristics within context of diffusion barrier and interfacial reactions. The Auger profiles after annealing at 600°C for 30 minutes in forming gas and after 50 hours at 500°C in air are shown in figures 4a and b, respectively. Generally, the two figures are similar in terms of phenomenological changes taking place within the layers. Figure 4a shows the unidirectional migration of silicon preferentially into platinum and toward the surface. This is of significant importance as it forms the basis of the diffusion barrier characteristics of the metallization. This migration creates a silicon-depleted zone inside the metallization as depicted in figure 4b. The AES profiles of figure 4 shows a build-up of consistently near 2:1 ratio of platinum to silicon within the platinum layer. Since we anticipate stable titanium silicide and carbide as the reaction products between titanium and SiC, no new source of silicon exists that will migrate to the surface. Although no strong indications of titanium carbide and silicide signals were observed at the epilayer interface, the extension of the contact boundary a few nanometers into the epilayer strongly suggested an underlying physical and chemical reaction.

An understanding of these chemical reactions can be seen in previous works by Bellina and Chamberlain [12,13]. The temperatures in which we performed the heat treatments were in the range of that of Chamberlain's work, who identified the formation of titanium carbide and silicide at similar temperatures. Applying Chamberlain's parabolic rate relation gives an approximation of the minimum thickness of reaction products:

$$x^2 = x_o + 2k(t - t_o) \text{ [cm}^2\text{]} \quad (2a)$$

$$k = k_o \exp\left(\frac{-262.7 \text{ kJ mol}^{-1}}{RT}\right) [\text{cm}^2 \text{s}^{-1}] \quad (2b)$$

where k_o is the reaction rate constant ($\text{cm}^2 \text{s}^{-1}$), k is the temperature dependence of the rate constant, x_o and t_o are initial distance and time constants, which in our case were set to zero, and R is the universal gas constant ($8.314 \text{ J} \cdot \text{mol}^{-1} \text{K}^{-1}$). Without correction for pressure, a layer of no less than 2nm of new products would have formed at the epilayer interface after 30 minutes of anneal at 600°C . While in-depth analysis is on-going, thermodynamic and reaction-limited kinetics are tentatively proposed to be acting in sequence, such that the decomposition of TaSi_2 in the presence of platinum proceeds with a final reaction written as follows:



If this reaction proceeds to the right, the limiting reactant would be silicon, since it is fully consumed by platinum. This proposition is made more likely given that the heat of formation of Pt_2Si ($-\Delta H_f \sim 10 \text{ kcal mol}^{-1}$) is less than that of TaSi_2 ($-\Delta H_f \sim 28 \text{ kcal mol}^{-1}$) [14]

It is very important to examine the oxygen concentrations in figure 4. Both figure 4a and 4b show very little migration of oxygen into the metallization. This implies a much more stable contact structure than previous scheme [10], which were affected by significant oxidation of the metals in the contact. Various groups have extensively studied the oxidation kinetics of the silicides. Murarka [15] concluded that the oxidation mechanism for most silicides essentially have the same heats of formation as normal oxides. Lie and Razouk [16,17] confirmed the oxidation kinetics of tantalum disilicide to have a parabolic rate constant. The implication is that it would take an appreciable length of time for oxygen to diffuse through the entire contact. In the future we plan to report extensively on the oxidation and decomposition characteristics of this metallization scheme within the context of long term reliability of high temperature ohmic contacts.

CONCLUSIONS

We have successfully demonstrated highly thermally stable ohmic contacts with low specific contact resistance. Three main issues that are still under study are the decomposition mechanism of tantalum silicide and its subsequent out-diffusion. Another is the reaction kinetics at the surface of the metallization. Last are the thermochemical reactions occurring at the TaSi_2/Ti interface. These are geared toward quantifying the active parameters that are specific to this scheme. The most important thing to note is that the penetration of oxygen to the interface of SiC was successfully arrested in the temperature range where SiC devices would operate. Oxidation of contacts and runaway reaction at the semiconductor interface, in general, remains a major reliability issue for wide bandgap devices that are expected to function in harsh environment. This work essentially established the foundation upon which future research efforts would be based.

ACKNOWLEDGEMENTS

We would like to thank the following individuals for making this work a reality: Drs. Jih-Fen Lei, Gary Hunter, and Phil Neudeck for their technical support. NASA and the Glennan Microsystems Initiative (GMI) funded this work.

REFERENCES

1. J.R. Bromstead, G.B. Weir, R.W. Johnson, R.C. Jaeger, and E.D. Baumann, Proc. 1st Intl. High Temp. Elec. Conf., p. 27-35, (1991).
2. R. Lee, G. Trombley, B. Johnson, R. Reston, C. Havasy, M. Mah, and C. Ito, Proc. 2nd Intl. High Temp. Elec. Conf., p. V3-8, (1994).
3. C. Passow, B. Gingerich, and G. Swenson, Proc. 4th Intl. High Temp. Elec. Conf., p. 219-221, (1998).
4. J.W. Palmour, H.S. Kong, D.G. Waltz, J.A. Edmond, and C.H. Carter, Jr., Proc. 1st Intl. High Temp. Elec. Conf., p.511, (1991).
5. R.F. Jurgens, IEEE Trans. on Industrial Electronics, **1E-29**, (2), p. 107-111, (1982).
6. J.S. Shor, R.A. Weber, L.G. Provost, D. Goldstein, and A.D. Kurtz, J. Electrochemical Soc., **141** (2), p. 579-581 (1994).
7. S. Liu, K. Reinhardt, C. Severt, J. Scofield, M. Ramalingam, and C. Tunstall, Sr., Proc. 3rd Intl. High Temp. Elec. Conf., p. VII (9-13), (1996).
8. N.A. Papanicolaou, A.E. Edwards, M.V. Rao, A.E. Wickenden, D.D. Koleske, R.L. Henry, and W.T. Anderson, Proc. 4th Intl. High Temp. Elec. Conf., p. 122-127 (1998).
9. Cree Research, Durham, NC.
10. R.S. Okojie, A.A. Ned, A.D. Kurtz, and W.N. Carr, IEEE Trans. Electron Devices, **46** (2), pp. 269-274 (1999).
11. E. Kuphal, Solid State Electronics, **24**, pp. 69-78, (1981).
12. J.J. Bellina, Jr., M.V. Zeller, in Novel Refractory Semiconductors, edited by D. Emin, T.L. Aselage, and C. Wood (Mater. Res. Soc. Symp. Proc. 97, Pittsburgh, PA, 1987), p. 265.
13. M.B. Chamberlain, Thin Solid Films, **72**, 305-311 (1980).
14. H.K. Henisch, Semiconductor Contacts: An approach to ideas and models, International Series of Monographs on physics no. 70. (Clarendon Press, Oxford, 1984).
15. S.P. Murarka, J. Vac. Sci. Technol., **17**, (4), Jul./Aug., p. 775-792 (1988).
16. L.N. Lie, W.A. Tiller, and K.C. Saraswat, J. Appl. Phys., **56**, (7), p. 2127-2132 (1984).
17. R.R. Razouk, M.E. Thomas, and S.L. Pressaco, J. Appl. Phys., **53**, (7), p. 5342-5344 (1982).